Introduction

Abstract

An optical coherence imaging diagnostic is being commissioned for time-resolved measurements (~ 10 ms) of ion emissivity, velocity, and temperature in the Compact Toroidal Hybrid (CTH) experiment. The Coherence Imaging (CI) technique measures the spectral coherence of an emission line with an imaging interferometer of fixed delay. CI has a number of advantages when compared to dispersive Doppler spectroscopy, including higher throughput and the capability to provide 2D spectral images, making it advantageous for investigating the non-axisymmetric geometry of CTH plasmas. A spectral survey of the visible and ultraviolet emission for a range of CTH discharges has identified helium and carbon impurity lines that will be utilized for CI measurements in CTH. First CI measurements of He II (468.6 nm) emission from CTH plasmas will be presented along with interferograms from a calibration light source and details of the instrument design. Results from this diagnostic will aid in characterizing the equilibrium ion parameters in both the edge and core of CTH plasmas for planned island divertor and MHD mode-locking experiments.

Compact Toroidal Hybrid (CTH)

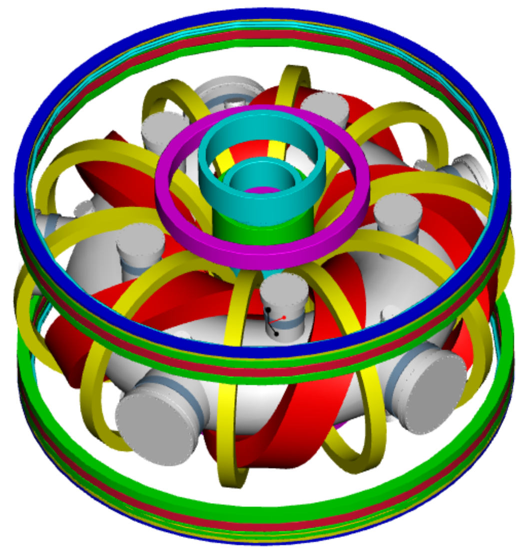

- CTH is a stellarator/tokamak hybrid device with an array of magnetic coils (helical, toroidal, poloidal, ohmic) providing access to a broad range of magnetic configurations
- A primary objective of the CTH program is to investigate the plasma stability when applying significant 3D magnetic shaping to current-carrying plasmas
- CTH serves as an excellent platform for the development of 3D equilibrium reconstruction, yielding enhanced understanding and predictive capability

Parameter	Range
R_0	0.75 m
a_{vessel}	0.29 m
a_{plasma}	≤ 0.20 m
I_p	≤ 80 kA
$\lvert B \rvert$	≤ 0.7 T
t_{vac}	0.02 to 0.32
T_e	≤ 200 eV
n_e	$\leq 5\times10^{19}$ m^{-3}
P_{ECRH}	≤ 30 kW

- Internal equilibrium measurements needed to understand MHD stability in 3D geometry
- Many core plasma parameters are reconstructed from edge measurements using the V3FIT[2] equilibrium solver
- Measurements of ion parameters in both the edge and the core of CTH plasmas beneficial for island divertor and MHD mode-locking experiments

Coherence Imaging

- Accurate measurement of interference pattern parameters provides information about the spectral emission (Doppler broadening and shift)

Advantages Compared to Dispersive Spectroscopy

- High-throughput due to no requirements of apertures or slits
- Possible to capture an entire two-dimensional image of emission and extract spectral information at each point in the image
  => Important for fully 3D plasma geometries such as CTH
- Possible extension to measure the spectral components of Zeeman splitting potentially yielding line-integrated magnitude and orientation of the magnetic field

Optical Schematic

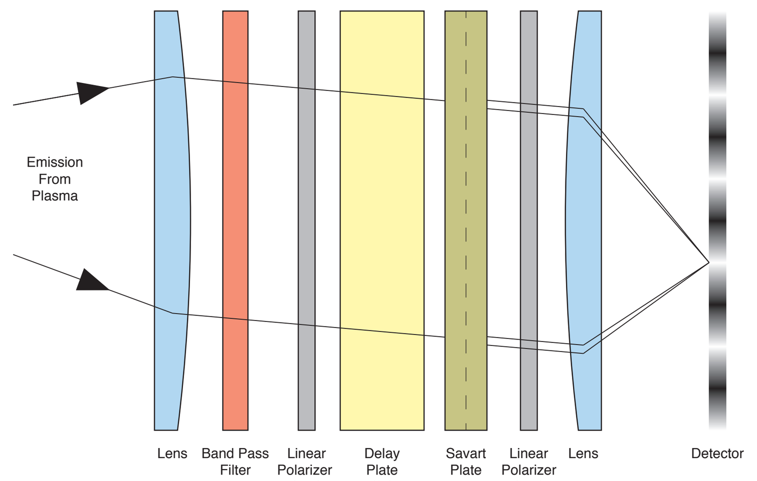

Collection Lens: collimates plasma emission from a wide angle into the diagnostic

Band-Pass Filter: selects a particular spectral line corresponding to an ion charge state of interest

Linear Polarizer: assures that transmitted emission is equally comprised of orthogonal polarizations (needed for maximum fringe contrast of interferogram)

Delay Plate: delays components of emission with orthogonal polarizations relative to each other (birefringence) on the order of ~1000 wavelengths (needed to provided sufficient measurement sensitivity)

Savart Plate: composite of two birefringent plates with optical axes oriented 90° to each other. Effect is to slightly delay orthogonal polarizations of emission relative to each other as a function of incident angle (relative to the Savart plate). Therefore, emission from different vertical locations in the plasma have slightly different delays between orthogonally polarized components.

Final Polarizer: detects total relative phase shift between the orthogonally polarized emission components (a rotation of the total polarization vector) due to both crystals (delay plate plus Savart plate).
  => *Produces horizontal fringe interferogram*

Second Lens: focuses transmitted emission onto the image plane

Detector: captures emission with overlaid interference pattern in time (fast camera)

Interpreting the Interferogram

- Doppler shift of a spectral line (velocity) observed as a change in the fringe spacing of interferogram
- Doppler broadening of a spectral line (temperature) observed as a modulation of the fringe contrast
- Measured fringe pattern from plasma compared to calibrated fringe pattern from known light source to determine Doppler shift and broadening

Instrument Specifications

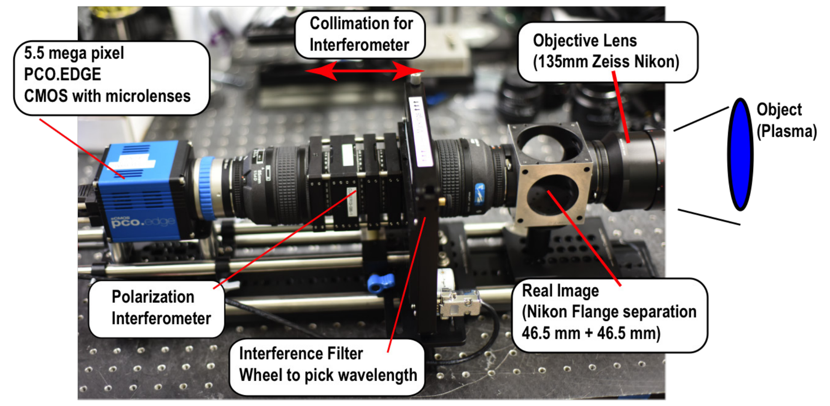

- Reversed F-mount lenses used collect emission from a wide angle and pass it through the polarization interferometer parallel. Image of first collection lens placed at detector plane the second lens.
- Polarization interferometer assembled from 2” optical components

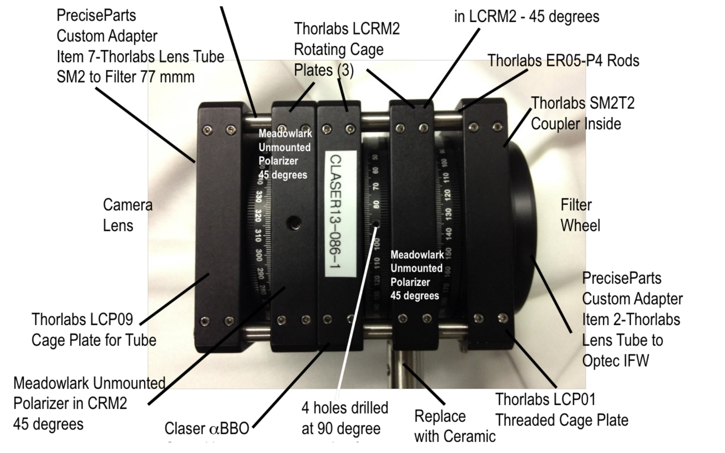

- Delay plate and Savart plate integrated into a single birefringent αBBO crystal (60 mm thick)
- Phase delay provide by αBBO crystal is sensitive to temperature variations. Therefore, interferometer surrounded by low power heaters and insulation for temperature feedback control to ~0.001 °C.

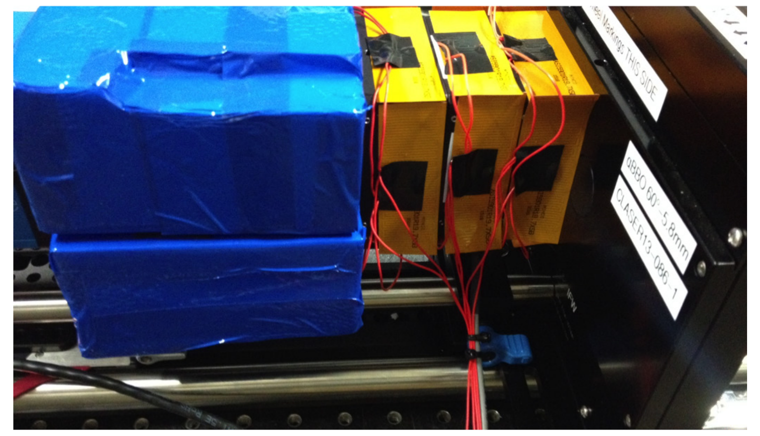

- Coherence imaging instrument installed on the CTH midplane

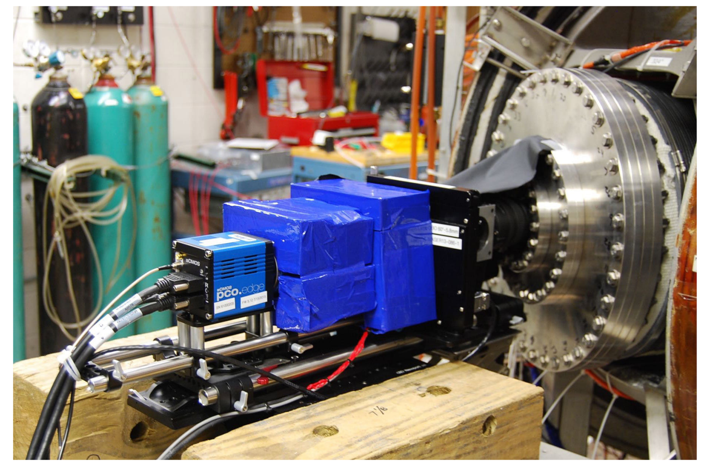

Instrument Calibration

Spectral Survey

- Selection of a robust spectral line for coherence imaging of CTH plasmas is critical to diagnostic feasibility
- Ideal spectral line would be located in the visible range, have a strong intensity over a broad range of CTH operating parameters and be free of other impurity lines
- Previous coherence imaging measurements have successfully used Ar II (488 nm)[3], C II (514.2 nm)[4,5], C III (464.9 nm)[4,5] & He II (468.6 nm)[5]
- Survey of potential impurity lines for various plasma conditions identified strong signals for He II (468 nm), C II (513), & C III (465 nm)

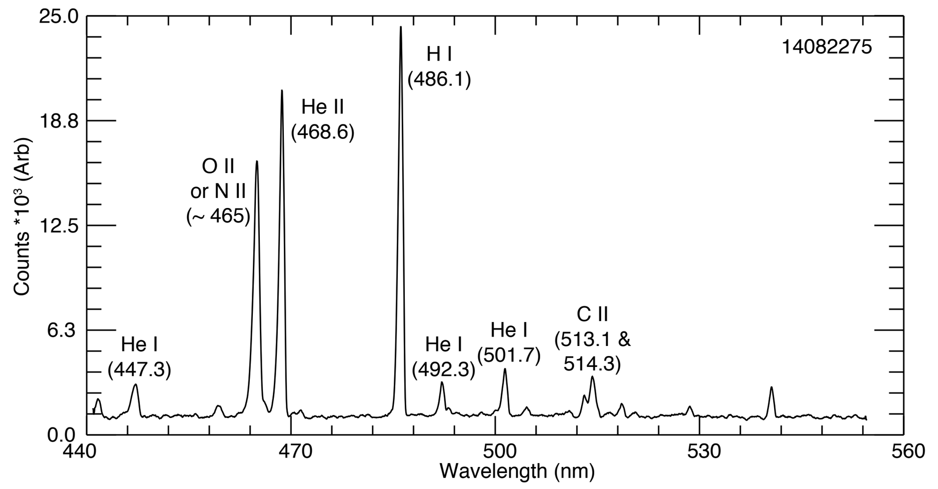

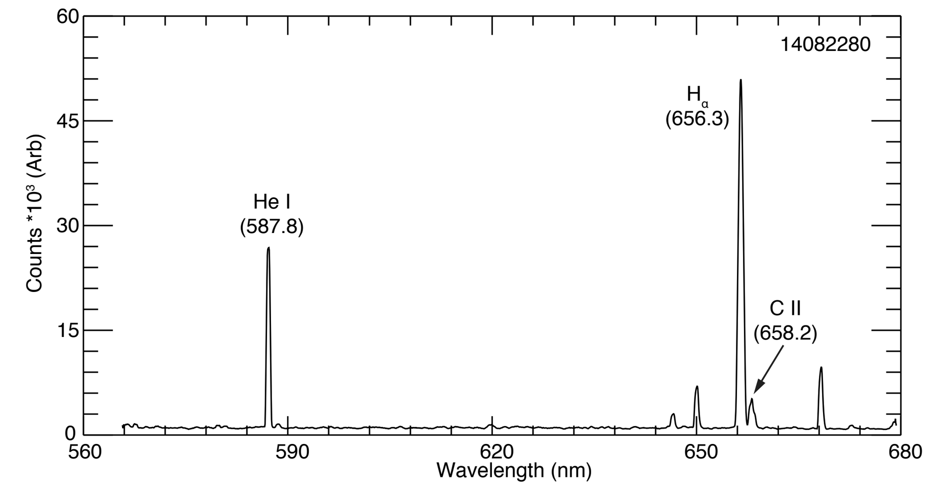

Calibrations

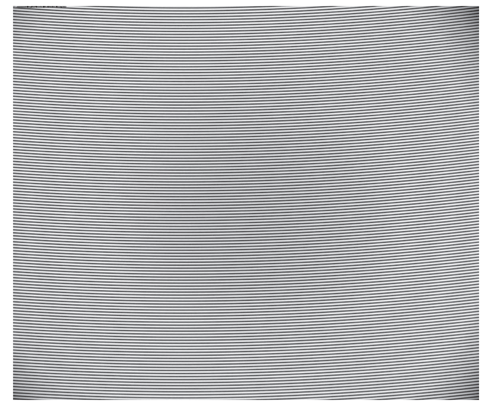

- Interferogram produced by instrument viewing Zn I emission at 465.0 nm
- With proper accounting, Zn I interferogram can be translated to the measured wavelength in the plasma and used a reference

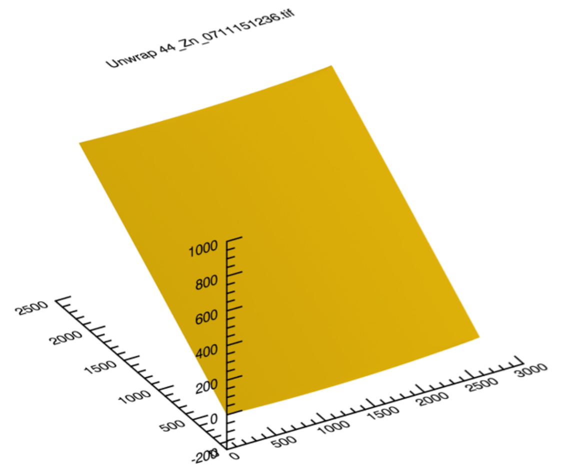

Initial Measurements

- First measurements with coherence imaging instrument produced strong fringes (high signal levels) for various impurity species He II (468 nm), C II (513), & C III (465 nm)

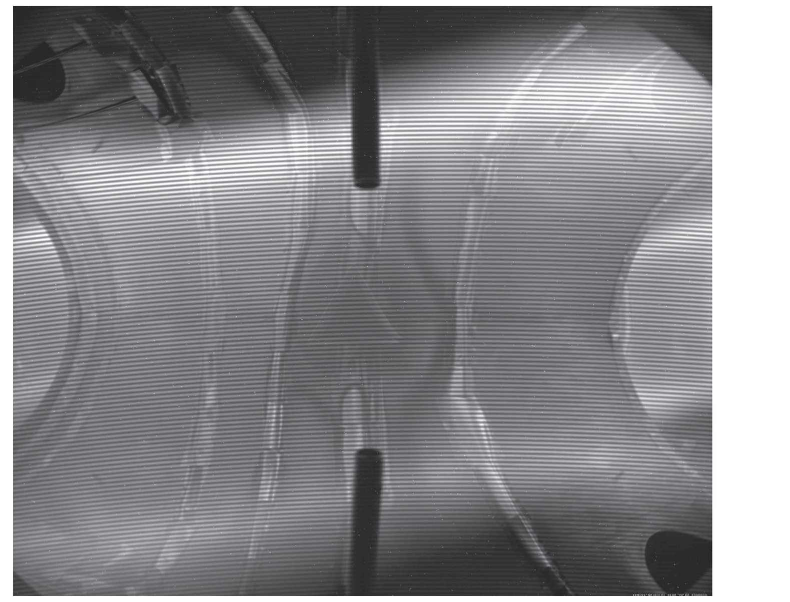

- Interferogram of C III emission at 465 nm during peak current with a 10 ms exposure

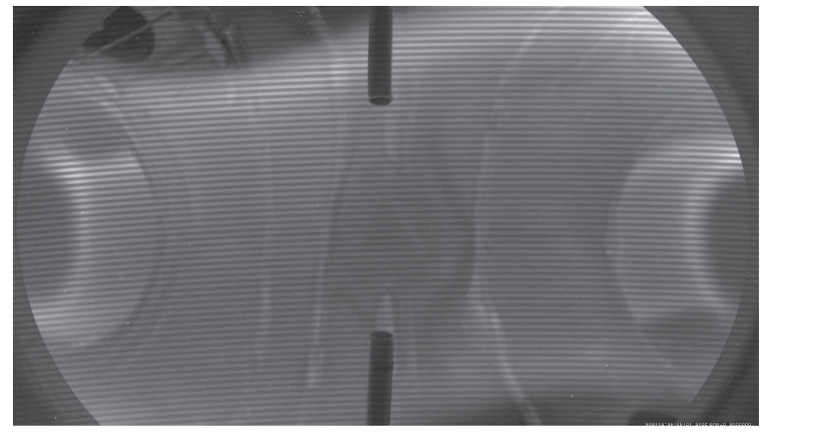

- Fisheye lens provides wide angle view of the interior of the vessel

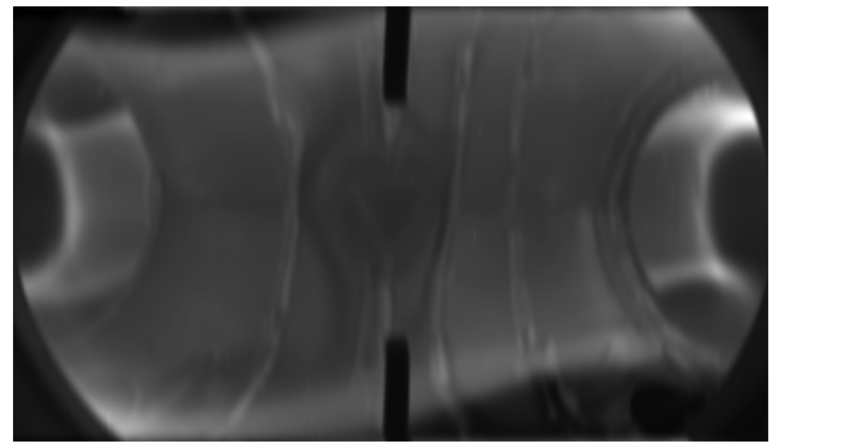

- Demodulated image (fringes removed)

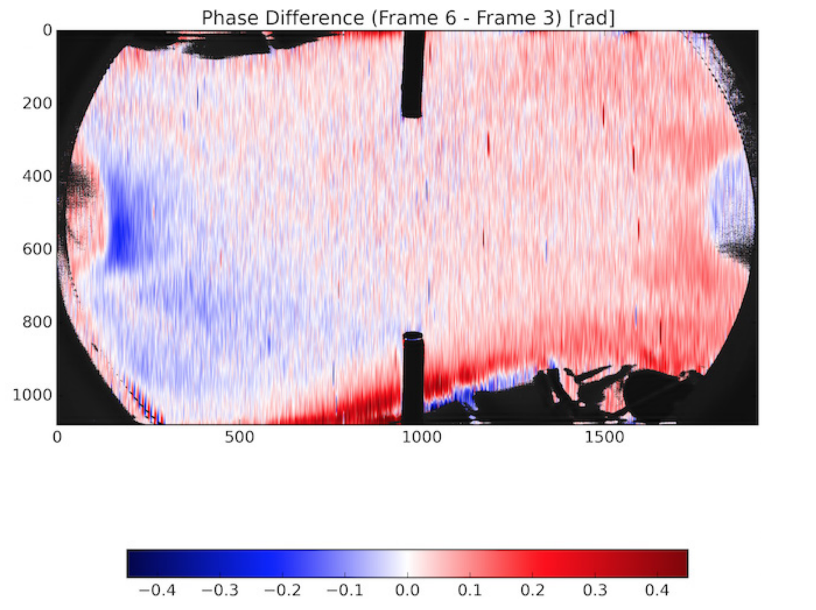

- Preliminary inversion calculated by subtracting a frame from early in the shot (low current) from a frame around the time of peak current suggests net toroidal flows on the order of 10 km/s (analysis by C. M. Samuell)

Conclusions

- New coherence imaging diagnostic designed and assembled for measurements of CTH plasmas
- Bench tests with calibration light sources (Zn I & Cd I) generate expected interferogram consisting of fringes with strong contrast
- Coherence imaging diagnostic successfully installed on CTH and commissioned in late July 2015
- First measurements of CTH plasmas reveal strong signals for a number of impurity species including C III (465 nm), He II (468 nm), & C II (513)
- Preliminary analysis of first measurements indicates net toroidal flows of on the order of 10 km/s

Future Work

- Incorporate calibration interferogram into diagnostic analysis for improved resolution of flow estimates
- Test different interferometer crystals for greater sensitive (larger delay) to detect smaller scale flows in CTH
- Continue to identify other strong emission lines over a range of operational conditions
- Modify hardware and analysis for impurity ion temperature diagnostics

References

[1]J. Howard, C. Michael, F. Glass, and A. Danielsson, Plasma Phys. Control Fusion., **45**, 1143 (2003).

[2]J. D. Hanson, S. P. Hirshman, S. F. Knowlton, L. L. Lao, E. A. Lazarus and J. M. Shields, Nucl. Fusion **49**, 075031 (2009).

[3]J. Howard, J. Phys. B: At. Mol. Opt. Phys. **43**, 144010 (2010).

[4]J. Howard, A. Diallo, M. Creese, S.L. Allen, R.M. Ellis, W. Meyer, M.E. Fenstermacher, G.D. Porter, N.H. Brooks, M.E. VanZeeland, and R.L. Boivin, Contrib. Plasma Phys. **51**, 194 (2011).

[5]S.A. Silburn, J.R. Harrison, J. Howard, K.J. Gibson, H. Meyer, C.A. Michael, and R.M. Sharples. Rev. Sci. Instr. **85**, 11D703 (2014).

Work supported by USDoE grant DE-FG02-00ER54610